MAGNETISM AND SUPERCONDUCTIVITY

The research related to magnetism is progressing steadily as shown by the number of new pertinent results of high quality at the international level and the large number of scientists involved coming from the Laboratoire Léon Brillouin and from other national and international laboratories. Let us mention as an example the "hot" result obtained recently which concerns the new rather unexpected discovery of **strong incommensurate magnetic fluctuations in the ruthenate** Sr_2RuO_4 (brother compound of the cuprate La_2CuO_4), a potent candidate for p-wave superconductivity.
The field covered is rich and in constant evolution with emergence of new subjects (spin ladders, ruthenates). The activities can be grouped into several subfields :
The first one (the largest) is entitled **Strongly Correlated Electron Systems**. After having got a strong impulse from the physics of high T_c cuprates, it progresses rapidly and becomes more unified. It includes the **Mixed Valence** and heavy fermions rare earth compounds, the **Low Dimensional** systems (spin Peierls system $CuGeO_3$ and spin ladder compound $(Sr,Ca)_{14}Cu_{24}O_{41}$), the "colossal magnetoresistance" **Manganites**, and naturally the **High T_c Cuprates** (and related materials such as the **ruthenates**).
The second one is the **Molecular Magnetism** developed in collaboration with the Chemistry group of O. Kahn at Bordeaux University.
The third one concerns **Magnetic Nanostructures,** a rapidly progressing theme which includes small agregates, superlattices and thin layered nanostructures.
The activity concerning **Magnetism in the frustrated Laves hydrides** $RMnH_x$ is rising rapidly .
Finally magnetic structure determination in various families of d and f intermetallic compounds constitutes an important activity in collaboration with several Solid State Chemistry Laboratories.

1. STRONGLY CORRELATED ELECTRON SYSTEMS

There are mainly two classes of strongly correlated electron systems : the rare earth (actinide) systems where the localised f electrons are strongly interacting with themselves and with the conduction electrons, and the d electron oxides where the d electrons are strongly interacting. Because of the strong interactions, Mott insulator-metal transitions are expected, new magnetic properties are obtained and Fermi liquid behavior of metals may break down. These strong interactions can lead to new types of superconductivity, charge and spin orderings. Neutron scattering is a good tool to study the new orderings and the fluctuations in their vicinity or at low dimension when ordering is suppressed and replaced by a **spin liquid** phase. This field is rapidly expanding both experimentally and theoretically. LLB takes part in this adventure.

1.a Mixed valence and Kondo systems (J.-M. Mignot)

This activity is developed by J.-M. Mignot together with postdocs in collaboration with French groups in Grenoble (Boucherle, Fak, Schweizer, Givord), a Russian group at Kourchatov Institute in Moscow (Alekseev, Clementyev, Goncharenko) and two Japanese groups, one at Tohoku University Sendai (Matsumara, Suzuki) and one at Tokyo Metropolitan University (Kohgi, Iwasa).

Antiferroquadrupolar order in TmTe

The most interesting result obtained in collaboration with the Japanese group at Sendai and with a postdoc (P. Link) is the determination by neutron diffraction of antiferroquadrupolar long range ordering in the mixed valence compound TmTe. This determination is indirect. Detailed information of the ordered state of quadrupolar moments is derived from the symmetry properties of the response to an applied magnetic field.

Mixed valence systems

In mixed valence systems such as Yb_4As_3 or Sm_3Te_4, the rare earth ion is not fluctuating between two valences but is either in one valence state or in the other. The number of ions in each valence state is fixed by charge neutrality. At low temperature, **charge ordering** occurs in Yb_4As_3. The ions with the valence corresponding to a magnetic ion order along one-dimensional chains which then behave as **spin 1/2 Heisenberg antiferromagnetic chains.** The excitation spin fluctuation spectrum has been studied by inelastic neutron scattering and the expected two-spinon

continuum spectrum has been recovered (in collaboration with the Tokyo Metropolitan University japanese group (Iwasa, Kohgi)).
In the other mixed valence system Sm_3Te_4, it seems that the different valence ions are not ordered even at very low temperature, but could form a **charge glass** with magnetic properties reminiscent of a spin glass of a new type (collaboration with Grenoble group : Boucherle, Givord, Schweizer).

Kondo systems
YbB_{12} is known to behave as a **Kondo insulator** with a small **charge gap** seen by photoemission. Neutron inelastic scattering on a powder sample have revealed a complex excitation spectrum with a well defined **spin gap**.
In heavy fermion systems (Kondo lattice) the border between the magnetic phase and the non-magnetic one is marked by the presence of a T=0 **quantum critical point (QCP)** which may be responsible for **non-Fermi liquid behavior**. The vicinity of such a QCP has been studied by inelastic neutron scattering in $Ce_{1-x}La_xRu_2Si_2$ with x close to .1 (collaboration with S. Raymond, L.P. Regnault, B. Fak (CENG)). The behavior seems to be different from another well studied compound $Ce(Cu_{1-x}Au_x)_6$ (Schröder)

1.b Low Dimensional systems
The renewal of interest in low dimensional systems is stimulated by the physics of high T_c cuprates for which the active electrons are located in D=2 dimensional CuO_2 planes and where **pseudogap** and non-Fermi liquid phenomena have been observed in the normal state, which are reminiscent of low dimensional electron systems (Luttinger liquid). Two quasi one-dimensional systems have been studied : the spin Peierls system $CuGeO_3$ and the spin ladder system $(Sr,La)_{14-x}Ca_xCu_{24}O_{41}$.

Spin Peierls system $CuGeO_3$
(M. Braden, B. Hennion, M. Ain (LLB), G. Dhalenne and A. Revcolevschi (Laboratoire de Chimie des Solides d'Orsay))
In this quasi one-dimensional system, the spin-Peierls dimerisation structural transition is based on the spin-phonon coupling. This aspect has been investigated in LLB for recent years by M. Braden. Contrary to the usual view which assumes an adiabaticity with fast magnetic excitations and slow phonons (soft modes), the situation has been shown to be the opposite. There are no soft modes, the phonons become harder so that there is non-adiabaticity. The spin excitations are slow and the phonon modes fast so that non-adiabaticity leads to a new effective spin Hamiltonian. This could explain (P. Pfeuty) the **recently discovered new excitation** by inelastic neutron scattering just above the two spinon continuum and independently of the spin-Peierls transition.

Spin Ladder system $(Sr,La)_{14-x}Ca_xCu_{24}O_{41}$
(L.P. Regnault (CENG), H. Moudden (LLB), J.E. Lorenzo (Laboratoire de Cristallographie de Grenoble)).
2-3-n legs ladders are one-dimensional systems which become closer to two dimensions when n becomes large. Such systems may constitute a link between one and two-dimensional electron systems and thus help to better understand the high T_c cuprate two dimensional physics. $(Sr,La)_{14-x}Ca_xCu_{24}O_{41}$ is a doped two-leg ladder system which becomes **superconductor** under pressure. The magnetic excitation spectrum has been studied by neutron scattering with clear evidence of a singlet-triplet excitation. Measurements as a function of doping show that the **spin gap** does not vary with doping. Experiments under pressure in the superconducting phase are expected soon. The samples are prepared by the Laboratoire de Chimie des Solides in Orsay (A. Revcolevschi)

1.c Manganites.
The oxides of perovskite structure with Mn ions have recently attracted a strong interest due to the discovery of a giant negative magnetoresistance. The doping of the family $RMnO_3$ (R: lanthanide) with divalent ions introduces holes in the d band that give rise to interesting interrelated magnetic, transport and structural properties.
Three projects are actually developed :

Inhomogeneities and magnetic excitations in $La_{1-x}Ca_xMnO_3$
(M. Hennion, F. Moussa, G. Biotteau [PhD student])
Pure $LaMnO_3$ is an insulator with a well defined antiferromagnetic structure at low temperature. When hole doping reaches a certain threshold around x=.3, the system becomes metallic and ferromagnetic and acquires new interesting transport properties. In order to understand this state, it is interesting to approach it from the low doping side $0<x<.2$. New unexpected properties have been discovered, some of which are not yet understood.
First, new **well defined low energy excitations** have been discovered from inelastic neutron scattering studies on single crystals (prepared by the Laboratoire de Chimie des Solides in Orsay).

Secondly, from small angle neutron scattering, **magnetic inhomogeneities** have been identified and characterized. These could be associated with **charge inhomogeneities** which are the object of much debate in the scientific community.
The same phenomena have been observed in the brother compound $La_{1-x}Sr_xMnO_3$.
Parallel studies (structural Jahn-Teller transitions) have been pursued on the same samples (J.Rodriguez-Carvajal).

Charge ordering phenomena
(J. Rodriguez-Carvajal, A. Daoud-Aladine [PhD student])
For specific doping elements and specific concentrations of these dopants a **charge ordered** state can be realized. This is the case for **$Pr_{.5}Ca_{.5}MnO_3$** and **$Nd_{.5}Ca_{.5}MnO_3$** which have been studied by neutron diffraction to reveal charge orderings (single crystals were grown by the Laboratoire de Chimie des Solides at Orsay). New experiments are planned with Ca replaced by Sr.
Another project leaded by C. Martin (Crismat-Caen; collaboration LLB: G. André, F. Bourée) deals with the relations between the nuclear and magnetic structures of some GMR manganites and their associated macroscopic (magnetic, transport...) properties. For the family $Pr_{0.5}Sr_{0.5-x}Ca_xMnO_3$ ($0<x<0.5$), the complete nuclear and magnetic phase diagram has been obtained from neutron powder diffraction showing the influence of the A cation size on the magnetic properties of the compounds. The influence of the doping on the Mn site on the charge and orbital ordering of the $Pr_{0.5}A_{0.5}Mn_{1-x}M_xO_3$ (A=Sr,Ca; M=Cr,Al; x=0.05) compounds has been studied for Cr and Al doping.

1.d Magnetism and Superconductivity in cuprates and ruthenates.

High T_c cuprates
LLB Neutron group (Y. Sidis [new CNRS recruitment], P. Bourges, D. Petitgrand, B. Hennion, M. D'Astuto [PhD student]), LLB Crystallogenesis group (G. Collin, P. Gautier-Picard [Postdoc], L. Manifacier [PhD student]), LLB Theory group (F. Onufrieva, P. Pfeuty, M. Kisselev [post doc], F. Bouis [PhD student]))
High T_c cuprates constitute the motor of the actual development of the field of strongly correlated electron systems. After more than ten years of intense experimental and theoretical efforts, the secrets of those highly complex electronic systems are still not yet unraveled and we should pursue our efforts.
High T_c cuprates are characterized by global anomalies : the very existence of high T_c anomalies observed for all properties in the underdoped regime above T_c, anomalies observed in the superconducting state. There are more and more arguments that all of them are somehow related to anomalous magnetism. This is why the study of details of magnetic properties becomes today a key point for understanding the physics of high T_c cuprates.
In LLB we follow a strategy combining three interrelated actions : **preparation** of large good quality single crystals; **inelastic neutron scattering** experiments giving access to the spatio-temporal magnetic response in both the normal metallic state and the superconducting state; **theoretical** developments trying to give a unified picture for both charge and spin properties.
The **underdoped** regime has been extensively studied. In the superconducting state, the existence of a **resonance peak** has recently been confirmed in a new system **$Bi_2Sr_2CaCu_2O_{8+\delta}$ (BiSCO),** in collaboration with B. Keimer and H.F. Fong (University of Princeton and MPI Stuttgart), for which the electronic spectra are known from photoemission experiments. The neutron resonance peak has larger momentum and energy width in BiSCO than in YBCO.
New experiments have been realized with **Zn** and **Ni** doped YBCO samples prepared by the LLB crystallogenesis group (G. Collin, P. Gautier-Picard). The effect of these two impurities seems to be rather different : Zn affects strongly the resonance peak, whereas Ni only shifts it slightly with a broadening in both wave vector and energy .
New results obtained in underdoped YBCO both in LLB and abroad (Mook, Hayden, Aeppli) show that for energy below the energy of the commensurate resonance peak there exists an **incommensurate** dynamic response. This has been explained by the LLB theory group (F. Onufrieva, P. Pfeuty) based on the general theory of two dimensional electron systems close to an Electronic Topological Transition (ETT). It is shown that the superconducting state in the two-dimensional electron system in the proximity of ETT (i.e. a long range ordered state with respect to charge degrees of freedom) is at the same time a **quantum spin liquid** state with respect to spin degrees of freedom and that both the resonance peak and the incommensurability are signatures of such a **mixed state**. As we already noticed, this is only part of a general theory developed by the theory group (F. Onufrieva, P. Pfeuty, M. Kisselev, F. Bouis). This theory being developed for different properties and for both normal and superconducting states allows to understand crucial anomalies observed experimentally in high T_c cuprates by NMR, inelastic neutron scattering, photoemission, tunneling... More generally it shed light on the nature of the new anomalous metallic state observed in the high T_c cuprates and on the very existence of high T_c superconductivity with d-wave symmetry.

Two other important situations remain to be understood : the **overdoped** regime for which actually no neutron scattering study exists; and the case of **electron doped** cuprates for which the phase diagram is different.
The electron doped system $Nd_{2-x}Ce_xCuO_4$ has been investigated (thesis submitted in 1998 by M.D'Astuto (under the direction of D. Petitgrand)). Samples were not good enough to study dynamic magnetic fluctuations in the superconducting state. The magnetism of rare earth Nd has been studied both in the pure non-superconducting sample Nd_2CuO_4 and in the superconducting sample (T_c=10K) $Nd_{1.85}Ce_{.15}CuO_4$. In Nd_2CuO_4, quasi-elastic scattering due to Nd has been measured with the existence of two components : a three dimensional one and a two dimensional one. This could be due to the nature of the interactions between the Nd and Cu ions. To better understand these interactions, magnetic excitations of Nd have been analysed at low temperature. In $Nd_{1.85}Ce_{.15}CuO_4$, magnetic order of Nd has been studied and it is shown that the effect of the presence of superconducting CuO_2 planes is to induce bidimensional order of Nd magnetic moments.
Finally the role of the reservoir planes in the high T_c cuprates has been considered in a recent PhD thesis work (L. Manifacier 1998 under G. Collin supervision) by crystallographic (structural refinements) and magnetic (diamagnetic susceptibility) studies performed on lead and rare-earth substitutions in Bi-2212 systems. The main conclusion reached is that "overdoped", "underdoped", and insulating phases would depend altogether on the carrier concentration in the CuO_2 planes, their mobility, and the physical state of the charge reservoirs.

Ruthenates
(M. Braden, W. Reichardt, (Kf. Karlsruhe) , Y. Sidis, P. Bourges, B. Hennion, G. André (LLB), Y. Maeno (Kyoto University))
A few years after the discovery of superconductivity in CuO_2 systems, a new **oxide superconductor** has been found : **Sr_2RuO_4**. This system has the same layered perovskite structure as La_2CuO_4, but behaves otherwise very differently. In its stoechiometric composition it is metallic and becomes superconductor at 1.5 K. The electronic properties are determined by the three 4d t_{2g} orbitals (d_{yz},d_{zx},d_{xy}) of the Ru^{4+} ion which form the bands that cross the Fermi level resulting in two electron-like quasi-one-dimensional Fermi Surfaces (FS) and one hole-like quasi-two dimensional FS (analogous to the 2D FS of cuprates). Some experiments suggest that superconductivity is rather unconventional of **p-wave symmetry** and could be due to the coupling with ferromagnetic fluctuations. To confirm this view it was essential to study the magnetic fluctuations by neutron scattering on a single crystal which was available (Maeno). Existing NMR results are difficult to interprete making neutron data essential. Recent results reveal unambigously intense dynamic **spin fluctuations** at low energy (8 meV) and for an **incommensurate** wave vector (.3,.3,0) $2\pi/a$. This can be interpreted in an itinerant picture as a dynamic quasi-nesting effect due to the two quasi-one dimensional electron like FS (Mazin, Pfeuty). These experiments have been made in the normal metallic state with temperature 10K<T<300K. Further experiments are planned to explore the superconducting state.
Lattice dynamics has been also explored. If the modes associated with an intra-plane charge ordering behave normally, an anomaly is observed for the vibrations associated with an inter-plane charge ordering .
When Sr is replaced by Ca, the system orders antiferromagnetically at low temperature. With excess oxygen, structural studies by neutron diffraction have shown that **Ca_2RuO_4** presents a first order structural transition associated with a metal-insulator transition.

2. MOLECULAR MAGNETISM

Molecular magnetism is at the borderline between magnetism and organic condensed matter chemistry. It constitutes an activity developed for many years in LLB by B. Gillon in collaboration with O. Kahn and his laboratory at the Institut de Chimie de la Matière Condensée in Bordeaux. Recently an English postdoc (John Stride) joined B. Gillon's group.
The main project developed actually consists in the study of the **ferromagnetic interaction mechanisms** in molecular compounds through the determination of the spin density map which is obtained from diffraction by polarized neutrons. The study of the organic radical triazole nitronyl nitroxide has not been completed because of the lack of sample. A complete study of the bimetallic compound **$MnNi(NO_2)_4(en)_2$** (en=ethylendiamine) has been realized. In this compound ferromagnetic chains are formed. The spin density map has been determined and the main result is the low apparent spin transfer from the metallic ions to the bridge NO_2 with a larger spin delocalization towards the outside atoms. This could be due to a compensation effect between two opposite effects, delocalization and spin polarization. Actually a similar study is in progress with the ferromagnetic bimetallic compound **$Mn_2H_2OMo(CN)_74H_2O$.**
The informations coming from spin density measurements are completed with charge density measurements from X-ray diffraction and compared to quantum chemistry calculations.

3. MAGNETIC NANOSTRUCTURES

Because of new fabrication tools (epitaxy, nanolithography), small size architectures are designed and a study of their fundamental properties is a challenge for future technological applications.

3.a Molecular nanomagnets : low energy excitations of the Mn_{12} acetate spin cluster

(I. Mirebeau, M. Hennion)

Molecular nanomagnets consist of a few (10-20) paramagnetic ions coupled by exchange interactions. The study of these large magnetic molecules has both fundamental and practical interest (information storage).

New data of very high precision concerning the low energy magnetic excitations of the Mn_{12} acetate spin cluster have been obtained by inelastic neutron scattering at LLB and ILL. This enables to separate the energy sublevels of the ground state and determine through a simple quantum mechanical calculation the value of a very small non- diagonal term which presence in the spin Hamiltonian is necessary to explain the excitation spectrum. This term which produces quantum tunneling between the different magnetic quantum levels is then responsible of the observed finite relaxation time of the magnetization at low temperature.

3.b Neutron Diffraction of rare earth superlattices and epitaxial films

(M. Hennion (LLB) and C. Dufour, K. Dumesnil, P. Mangin (Laboratoire de Physique des Matériaux, Nancy))

Spin reorientation in Laves phases (RE)Fe_2 (RE=rare earth).

Laves phases (RE)Fe_2 present a giant magnetostriction effect at room temperature with potential applications. An epitaxial film of the ternary compound $Dy_{.7}Tb_{.3}Fe_2$ has been prepared and studied by neutron diffraction to follow the spin reorientation as a function of temperature. An actual project concerns the polarized neutron study of the superlattice $DyFe_2/YFe_2$ to determine the spin density and follow the spin reorientation as a function of temperature and magnetic field.

Light rare earth films and superlattices

Neutron diffraction of Sm films with thickness of 4000 Å show that the magnetic order of the Sm in the hexagonal sites seems to be the same as in the bulk, but with a higher magnetic moment. The nature of long range interactions between magnetic Sm through non magnetic Nd phase should be studied on superlattices Sm/Nd.

3.c Magnetic structure of superlattices, thin films and regular nanostructures from polarized neutron specular and off-specular reflectometry and surface diffraction

(C. Fermon, F. Ott)

These three different techniques are developed at LLB. When applied together to regular magnetic nanostructures of sufficient size, they give a full 3D magnetic structure determination both parallel and perpendicularly to the surface of the nanostructure. These techniques have been applied to different examples of nanostructures : this necessitates large regular samples (1cm ×1cm) with repetitive motives (alternate lines, alternate layers, lattice of magnetic motives). Only a few laboratories prepare such samples and collaborate with the LLB : SPEC Saclay, CENG Grenoble, CRISMAT Caen, IEF Orsay, IPCMS Strasbourg. The systems studied are Fe/Mn/Fe sandwich structures, $(LaMnO)_m(SrMnO)_n$ superlattices, FePd and Co thin layers with magnetic domains, Pt/Co irradiated interfaces and M/Co/M (M=Au,Pt) sandwiches, Co/Mn superlattices, $La_{.7}Sr_{.3}MnO_3/SrTiO_3$ interface, $La(Sr,Ca)MnO_3/YBa_2Cu_3O_7$ interface, Si/SiO_2/Co systems with an electric field.

4. Magnetism in the frustrated Laves hydrides $RMnH_x$

(I. Mirebeau (LLB), I. Goncharenko and A. Irodova (Kurchatov Institute, Moscow))

The RMn_2 compounds where R is Y or a rare earth metal, have been studied during the recent years for several interests : the magnetism of Mn at the border between localized and itinerant; the interplay between R and Mn magnetism; quantum frustration effects for the Mn sublattice with antiferromagnetic interactions.

When hydrogen is added and occupies the interstitial site in the metal sublattices, new interesting effects can be studied : hydrogen acts as a negative pressure on the magnetism of Mn; hydrogen can order and the H ordering can affect the magnetic ordering of Mn and R.

In recent studies of the magnetic and crystal structures of **$YMn_2H_{4.3}$,** a peculiar interplay between the magnetic and hydrogen order has been observed. Mn magnetic moments and hydrogen atoms order simultaneously through a first order structural transition.

Further neutron diffraction (and eventually inelastic neutron scattering) studies of the interplay between hydrogen and magnetic orders are in preparation using chemical substitution, applied pressure and varying the hydrogen content.

Similar structural and magnetic phase determinations have been pursued on the same hydrides but for lower hydrogen concentration (specifically x=1.1) by M. Latroche, V. Paul-Boncour from CNRS-Thiais and F. Bourée, G. André (LLB).

5. DETERMINATION OF MAGNETIC STRUCTURES IN MAGNETIC SYSTEMS WITH D AND F ELECTRONS

When new families of magnetic compounds are synthesized, it is essential to determine their magnetic structure in order to have access to the microscopic magnetic interaction at work. This is done in close collaboration with solid state chemistry laboratories in France (Bordeaux, Rennes, Paris VI, Clermont-Ferrand...) and abroad (Spain, Germany, Poland, Russia, Switzerland). Many different compounds are studied, ranging from transition metal, rare earth to actinide compounds. Among these, let us consider three typical examples:
With the ICMCB Bordeaux (B. Chevalier) and the LLB (F. Bourée and T. Roisnel), the study of the family R_2T_2X (R=rare earth or U; T=transition metal; X=Sn or In) has been pursued (PhD thesis of D. Laffargue) mainly for X=Sn, T=Pd and R=Tb,Dy,Ho,Er. Two magnetic structures (commensurate and incommensurate) have been determined at low temperature for all of these four compounds but with different magnetic moments depending on the rare earth element and reflecting the competition between the magnetic RKKY exchange and the crystalline field anisotropy.
The magnetic structures of different and new Uranium compounds (UGe_2, U_3Ge_5, U_3TiGe_5, $U_3Ga_2Ge_3$) synthesized by the group of H. Noël at Rennes (collaboration with LLB (G. André and F. Bourée)) have been obtained, stressing the key role of the local Uranium ion environment (nature and ligand position in the cell) on the Uranium magnetic properties.
A study on a new Terbium fluoride family has begun with the compound KTb_3F_{12} (D. Avignant from Clermont-Ferrand in collaboration with the LLB (F. Bourée and G. André)) where Tb is present in two valence states : Tb^{4+} and Tb^{3+} (ratio $Tb^{3+}/Tb^{4+}=1/2$). Neutron diffraction gave two main results : the precise localization of the light F atoms leads to correct the X-ray space-group determination (from I4/mmm to I4/m); the compound is antiferromagnetic below $T_N \approx 3.65K$ with only the Tb^{4+} moments magnetically ordered.

CONCLUSION

Six years after the impulse given by Jean Rossat-Mignod when he joined the LLB from 1991 to 1993, the activity in magnetism is progressing well with a large spectrum of research themes.
It benefits from a close collaboration with chemists : O. Kahn (Bordeaux) for molecular magnetism, A. Revcolevschi (Orsay) for the preparation of single crystals of Strongly Correlated Electron Systems and G. Collin and P. Gautier-Picard (crystallogenesis group at LLB) for the preparation of single crystals of high T_c compounds.
Efforts are made to get better instruments (new polarized neutron triple-axis 2T) with a better environment (high pressure and high magnetic field).
The coupling with theory is good especially on high T_c cuprates and is progressively extending to other subjects.

SPIN DENSITIES IN FERROMAGNETIC MN(II)NI(II) BIMETALLIC CHAINS : POLARIZED NEUTRON DIFFRACTION

B. Gillon

Laboratoire Léon Brillouin (CEA-CNRS)

In the field of molecular magnetism, the determination of spin density maps provides crucial information about phenomena such as spin delocalization and spin polarization that play a role in magnetic interactions between metallic ions through organic bridges. The compound $MnNi(NO_2)_4(en)_2$ (with « en » = ethylenediamine) constitutes the first bimetallic ferromagnetic chain compound to be fully characterized, both magnetically and structurally. The chains present a zig-zag structure formed by alternating Mn(II) and Ni(II) ions bridged by a bidendate NO_2^- group, as shown by Figure 1. The two oxygen atoms of the bridging nitro group are linked to Manganese and the nitrogen atom is bonded to Nickel.

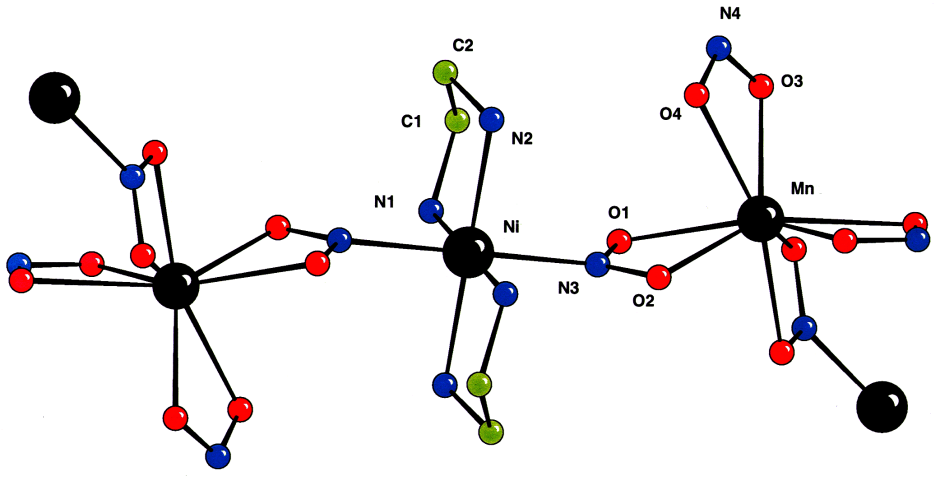

Figure 1 Structure of the chain in $MnNi(NO_2)_4(en)_2$ at low temperature from unpolarized neutron measurements at 20K on 5C2

The Nickel ion is located on an inversion center, in a nearly perfect octahedral environment. It is surrounded by four nitrogen atoms coming from the two ethylenediamine groups and by two NO_2^- bridging nitrogen atoms. The Manganese ion resides on a two-fold symmetry axis and presents an unusual coordination sphere consisting of eight oxygen atoms, with two non-bonding oxygen atoms at a slightly larger distance than the six others. The intrachain Mn ... Ni distance is equal to 4.817Å.

The structure can be described as a superimposition of ABAB layers perpendicular to the [001] direction: in the A layer the chains are parallel to [110] while in the B layer they are directed along the [-110] direction. Magnetic susceptibility measurements give evidence for a weak intrachain ferromagnetic coupling J = 1.33 cm^{-1}. A long range antiferromagnetic ordering between the chains occurs at T_N = 2.35K. The behaviour of the magnetization versus magnetic field is characteristic of a metamagnetic compound with a threshold field of 1.2 KOe.

Figure 2 shows the induced spin density map, in projection perpendicular to the N1-Ni-N3 plane. The spin density is positive over all the map including on the NO_2^- bridge. This map was obtained by a multipole model refinement on a set of 127 independent magnetic structure factors measured on the polarized neutron diffractometer 5C1 of the L.L.B. In this model the spin density is assumed to be the sum of atomic spin densities centered on the metal ions and on their first neighbours.. Spherical atomic spin densities were assumed for all atoms except Nickel, for which a 3d-type spin density was refined. The refined spin populations are normalized to 7 μ_B for each MnNi unit which corresponds to a system of local spins $S_{Mn^{2+}} = +5/2$ and $S_{Ni^{2+}} = +1$.

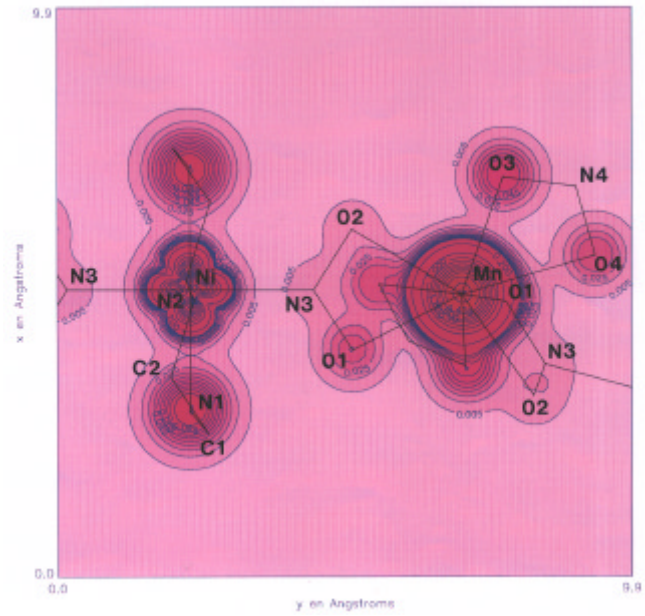

Figure 2 Induced spin density integrated along the perpendicular to the N1-Ni-N3 plane in the ferromagnetic chain compound $MnNi(NO_2)_4(en)_2$ at 4K under an applied field of 2 Teslas. Positive spin density is in red. Different intervals are used for the low density and high density levels: low levels (from 0.005 to 0.095 $\mu_B/Å^2$ by steps of 0.010 $\mu_B/Å^2$) and high levels (from 0.2 to 4.2 $\mu_B/Å^2$ by steps of 0.4 $\mu_B/Å^2$)

The Mn^{2+} and Ni^{2+} spin populations are respectively equal to 4.48(4) and 1.62(3) μ_B. The unpaired spin on Ni^{2+} is found to be essentially located in the $d_{x^2-y^2}$ and d_2x orbitals. For Mn^{2+}, equal populations of the five 3d orbitals were assumed. The quantity of spin transferred from Mn^{2+} to its neighbours only amounts to 8 per cent of the moment associated to the manganese region while the spin delocalization from Ni^{2+} represents 24 per cent of the total moment on the nickel site, reflecting the stronger covalent character of the nickel than that of the manganese ion.

The delocalization from the nickel ion towards the bridging N3 atom of the nitro group (0.01(3)μ_B) is clearly weaker than towards the atoms of the ethylenediamine groups N1 (0.16(3)μ_B) and N2 (0.09(3)μ_B). Similarly the spin transfer from Mn^{2+} is smaller on both oxygen atoms of the bridge O1 (0.04(3)μ_B) and O2 (0.01(2)μ_B) than on the O3 atom (0.08(2)μ_B) of the non-bridging NO_2^- groups. The weak spin population on the oxygen atom O4 (0.05(2)μ_B) may be explained by the larger Mn-O4 distance.

The apparently negligible spin transfer from both metallic ions towards the atoms of the NO_2^- bridging group, compared to the significant spin transfer towards the external ligands is quite paradoxical. The interpretation that we propose is a balance between two phenomena which act in opposite ways: spin delocalization responsible for s type positive spin density on the neighbours of the metallic ions and spin polarization responsible for negative spin density of p type on the second neighbours. On the spin density map, the positive spin actually delocalized from each metallic ion towards its first neighbours belonging to the bridge would then be compensated for by a negative contribution due to the presence of the other metallic ion.

Acknowledgments

The author thanks Professor O. Kahn, from the Institut de Chimie de la Matière Condensée de Bordeaux (I.C.M.C.B.), who initiated this work, C. Mathonière and T. Rajendiran (I.C.M.C.B.) for the single crystal elaboration and A. Cousson (L.L.B.) for the low temperature structural study.

[1]O. Kahn, E. Bakalbassis, C. Mathonière, M. Hagiwara, K. Katsumata and L. Ouahab, Inorg. Chem. **36** (1997) 1530.
[2]E. Ressouche, A. Zheludev, J.X . Boucherle, B. Gillon, P. Rey and J. Schweizer, Mol. Cryst. Liq. Cryst. **233** (1993) 13.

OBSERVATION OF A FERROMAGNETIC MODULATION IN DOPED MN PEROVSKITES: AN ELECTRONIC PHASE SEPARATION

G. Biotteau[1], M. Hennion[1], F. Moussa[1], J. Rodriguez-Carvajal[1], L. Pinsard[2] and A. Revcolevschi[2]

[1]Laboratoire Léon Brillouin, CEA-CNRS,
[2]Laboratoire de Chimie des Solides, Université Paris-Sud, 91405 Orsay Cedex, France

In manganites $La_{1-x}A_xMnO_3$, where the divalent ions (A=Sr, Ca, Ba) induce a hole doping, the coupling between the hole mobility and the ferromagnetism provides spectacular effects. Close to the magnetic transition where the metal-insulator transition occurs, an applied field induces a variation of the resistivity by several orders of magnitude (giant magnetoresistance), the largest effect being for x≈0.3. On a fundamental basis, the parameters leading to these effects are still not clearly understood. For several years, the existence of magnetic inhomogeneities has been suggested[1-3], associating the ferromagnetic transition and likely the metal-insulator transition to a percolation effect. Several experiments[4-5] have reported unusual fluctuations close to the ferromagnetic transition $T \approx T_c$, suggesting a picture of fluctuating ferromagnetic clusters.

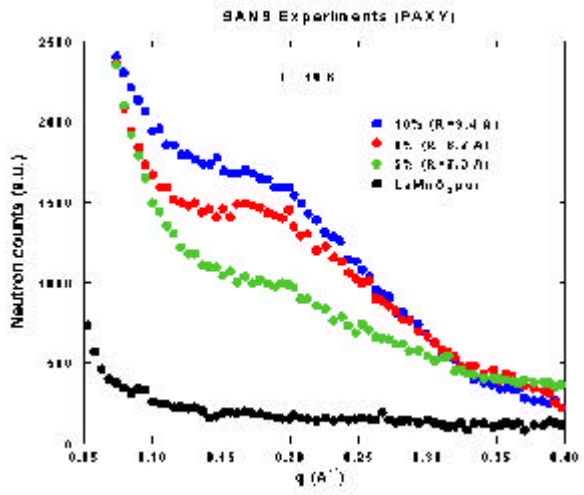

Figure 1. Scattering Intensities versus q observed using the diffractometer PAXY with an incident wavelength λ=6Å for x=0, 0.05, 0.08, and 0.1 of Ca doping. The intensities, renormalised by the volume, taking account of the sample transmission are readily comparable.

We have undertaken a small angle scattering study, using a small angle diffractometer (PAXY) in a first step, and then, a three-axis spectrometer (4F1), in an elastic configuration. The first one (PAXY), thanks to the multidetector device, provides measurements with an isotropic q resolution. However, any static (ω=0) spin correlations cannot be observed as a function of temperature (contamination by the spin excitations) so that the magnetic contribution cannot be separated from the nuclear one. By contrast, the three axis spectrometer allows to determine any ω=0 scattering intensity at any temperature, and, by subtracting the nuclear contribution determined at high temperature, allows to select the purely magnetic contribution.

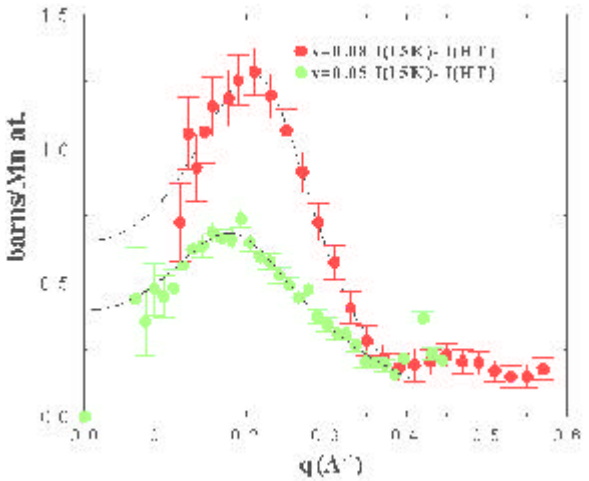

Figure 2. Scattering Intensities of magnetic origin, $I(q)=I_{15K}-I_{HT}$, versus q, calibrated in barns per Mn atom, observed using a three axis spectrometer for x=0.05 and x=0.08. The dashed line is a calculated curve according to the model described in the text

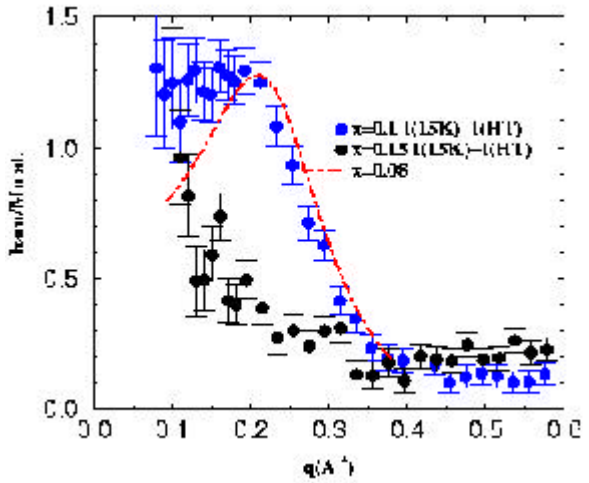

Figure 3. Scattering Intensities of magnetic origin $I(q)=I_{15K}$ - I_{HT}, versus q, calibrated in barns per Mn, observed using a three-axis spectrometer for x=0.1 and x=0.15. The dashed line is a guide for the eye.

In the 0≤x≤0.15 range studied, both experiments reveal the occurrence of a ferromagnetic modulation, in all the q directions. We have shown that it can be interpreted in terms of magnetic inhomogeneities,

with a liquid-like distribution, and therefore in repulsive interaction. Both the size of the inhomogeneities and their characteristic distance can be quantitatively determined. Such an experimental result, observed for the first time, likely originates from a purely electronic effect[6].

In the range $0 \leq x \leq 0.15$, the compounds are insulating at all temperatures and, depending on x, undergo either a transition from a paramagnetic to a canted-antiferromagnetic state at T_{CA} (T_{CA}=122K at x=0.08) or a transition from a paramagnetic to a ferromagnetic state at T_C=155K for x=0.15.

In figure 1, the SANS scattering intensities obtained at 10K for x=0, 0.05, 0.08 and 0.1 are compared. The new experimental feature occurring in doped samples is a q-modulation, growing with x and superposed on a large scattering intensity (see the weak scattering intensity in the pure $LaMnO_3$). The multidetector device allows in principle, to check the q-isotropy of this modulation, but here, the complication related to the twinning domains prevents any definitive conclusion. A similar study on a three-axis spectrometer allows to separate the contribution of nuclear origin (dislocations or any structural defects induced by Ca doping) determined above the magnetic transition T_{CA}, where the intensity I(q) is temperature independent, from the intensity of magnetic origin that grows below T_{CA}. This magnetic contribution is reported in figure 2 at 15K, for x=0.05 and x=0.08 of Ca. It reveals clearly that the modulation observed around $q \approx 0.2 Å^{-1}$ using PAXY has a magnetic origin and its intensity evolves strongly in this small concentration range. The magnetic contribution is also shown at higher doping value in figure 3. At x=0.1 the scattering intensity is close to that observed for x=0.08 (represented by the red dot-dashed line) except at small q, where a flat plateau instead of a true modulation is observed. At x=0.15, the modulation is no more observed in our experimental window . We have also studied the temperature evolution of the scattering. In figure 4 , the evolution with temperature observed in the sample with x=0.05 is reported. It shows that as the intensity decreases, there is a slight shift of the modulation towards smaller q values. Since the studied samples are single crystals, all the experimental features observed close to the direct beam also exist around Bragg peaks. For example, in Figure 5, the intensity observed around (110) Bragg peak is reported for x=0.08 at several temperatures. There, the q-modulation is clearly observed, without any subtraction. It disappears above the magnetic transition (T_{CA}=122K), where a monotoneous decreasing scattering intensity, nearly temperature independent, persists. In addition, a study at small angle scattering using X-rays, for which a large contrast between La and Ca scattering exists, has been performed. It allows to check that there is no scattering in this small q range, which excludes any chemical clustering related to Ca impurities associated to the magnetic scattering observed by neutrons.

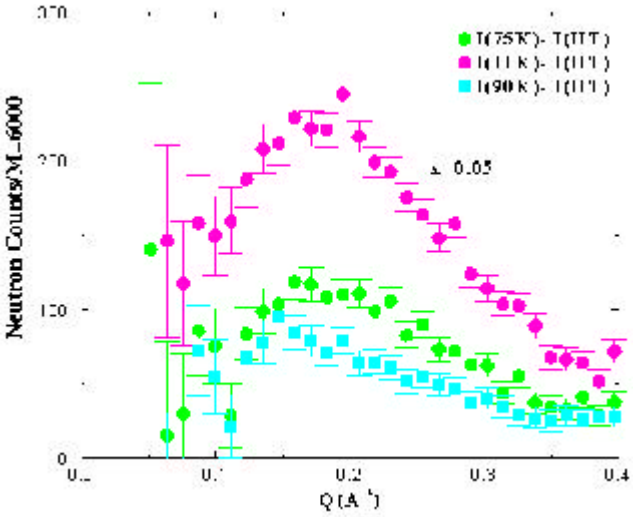

Figure 4. Diffuse scattering intensity versus Q along [110] at several temperatures obtained at x=0.08 of Ca doping.

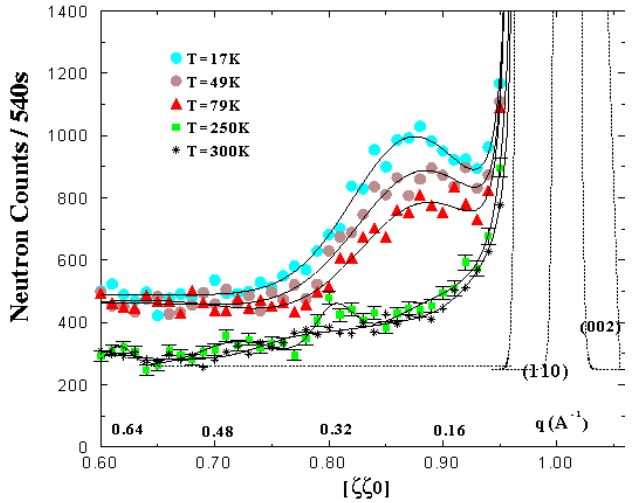

Figure 5. Diffuse scattering intensity versus Q along [110] at several temperatures obtained at x=0.08 of Ca doping.

The existence of such an isotropic modulation, suggests a typical characteristic distance between similar magnetic inhomogeneities as in a liquid-like distribution. These inhomogeneities can be seen thanks to the contrast between their magnetization density and that of the surrounding matrix. To get a more quantitative description, a hard sphere model has been used with a liquid function for the distribution and excluded volumes, assuming a perfect isotropy. The corresponding calculated curves which fit the experimental data are shown also in Figure 2 for x=0.05 and x=0.08. They determine a typical size of 15 Å for x=0.05, increasing to 18 Å for x=0.08 with a typical distance of 38 Å. The most striking result is that the density of these inhomogeneities, or "droplets", is smaller by more

than an order of magnitude than the density of Ca atoms. Such a result gets rid of a picture of magnetic polarisation surrounding each Ca or hole defects, but rather suggests a purely electronic effect of hole rich regions in repulsive interaction within a hole poor medium. This segregation would occur on a small spatial scale of some tens of Å. The temperature dependence reported for x=0.05 reflects a decrease of the size of the inhomogeneity and of their spatial density. However, the fall down of the intensity may be also related to a change of the magnetic contrast which must become nul in the paramagnetic state. The calibration of the intensities in barns per Mn atom, allows in principle, an estimation of the difference between the magnetization densities of the two magnetic regions at low temperature. This determination is model dependent. In particular, the isotropy of the structure, which could not be checked with accuracy because of twinned domains, is assumed.

The present determination of the magnetic contrast, 0.7 μ_B, does not agree with a ferromagnetic state within the hole rich regions. This conclusion apparently disagrees with NMR experiments performed on the same samples. These latter experiments indicate that some Mn spins follow the applied field as expected for spins within a ferromagnetic state. Both findings can be conciliated in a more complex picture of magnetic clusters with a small ferromagnetic core, therefore not observable by neutrons (the intensity is proportional to the square of the volume).

Very recently, a similar study has also been performed in a x=0.06 Sr doped compound. A ferromagnetic modulation with characteristics close to those found for Ca doping has been also observed. This suggests the general character of these observations.

The disappearance of the modulation in the scattering intensity for x=0.15, where the compound is fully ferromagnetic, could be explained by a percolation of the magnetic inhomogeneities or by an homogeneization of the electronic density. In the first case, one expects the intensity to be restricted within a much smaller q scale, out of the present experimental window.

The role of such an electronic phase separation in the metal-insulating transition, is still unclear. At x=0.15, where one can expect a percolation of these inhomogeneities, the compound keeps insulating properties. This stresses out that the magnetic state alone is insufficient to explain the metal-insulating transition.

References

[1] E. L. Nagaev, Phys. Status Solidi B **186**, 9 (1994)

[2] M.Kagan, M.Mostovoy and D.Khomskii, cond-mat/9804213 Los Alamos April 1998

[3] S. Yunoki, J. Hu,A.L. Malvezzi, A. Moreo, N. Furukawa and E. Dagotto, Phys. Rev. Lett. **80**, 845 (1998)

[4] J. M. De Teresa M. R. Ibarra, P. A. Algarabel, C. Ritter, C. Marquina, J. Blasco, J. Garcia, A. Del Moral, Z. Arnold, Nature **386**, 256 (1997)

[5] J. W. Lynn, R. W. Erwin, J. A. Borchers, Q. Huang and A. Satoro, Phys. Rev. Lett. **76**, 4046 (1996)

[6] M. Hennion, F. Moussa, G. Biotteau, J. Rodriguez-Carvajal, L. Pinsard, A. Revcolevschi, Phys. Rev. Lett. **81**, 1957 (1998)

INTERPLAY OF ANTIFERROQUADRUPOLAR AND ANTIFERROMAGNETIC ORDER IN TmTe

P. Link[1], J.-M. Mignot[1], A. Gukasov[1], T. Matsumura[2] and T. Suzuki[2]

[1]Laboratoire Léon Brillouin (CEA-CNRS)
[2]Tohoku University, Sendai, Japan

Neutron diffraction is the reference technique for probing long-range order formed on a lattice of atoms or magnetic moments. It is shown that, under certain conditions, it can also be invaluable for studying more exotic types of ordered structures involving electron charge distributions. Although the determination is indirect in this case, detailed information on the ordered state of quadrupole moments can be derived from the symmetry properties of the response to an applied magnetic field. This method is demonstrated in the case of the antiferroquadrupolar phase of TmTe.

Besides their magnetic dipole moments, lanthanide elements with incomplete 4*f* electron shells are known to also possess higher-order moments (quadrupole, octupole, etc.). In a classical picture, this reflects the non-sphericity of the electron charge distribution. In the case of solids, pair interactions between 4*f* quadrupoles located at neighboring sites can occur either directly through their electrostatic potentials (usually weak), or indirectly through various channels such as lattice strains (cooperative Jahn-Teller effect), conduction electrons in metals (RKKY-type coupling), higher-order exchange terms, etc. For most real systems, conventional magnetic interactions dominate, and the 4*f* dipole-moment lattice orders in a long-range magnetic structure at low temperature. Accordingly, the quadrupole moments will have non-zero values in the magnetic state, but this is only the result of dipole ordering. More rarely, quadrupole interactions can prevail and produce a phase transition on their own, whose primary order parameter is a component, or combination of components, of the quadrupole moment tensor. In some intermetallic compounds (TmZn, CeAg), as well as in typical Jahn-Teller systems (rare-earth zircons), the value of the order parameter is uniform at all sites, and the order is thus denoted "ferroquadrupolar" in analogy with magnetism. On the other hand, staggered types of quadrupole order, loosely termed "antiferro-quadrupolar" (AFQ), have been reported so far only for a small number of metallic compounds ($TmGa_3$, CeB_6). However, their study is of particular interest because the tensor nature of the quadrupole moment operator, as well as the possible interplay between magnetic and quadrupole order parameters, may result in a rich variety of physical situations. To characterize these phases, microscopic information is even more crucial than in the case of magnetism because one has to determine not only the wave-vectors and Fourier components of the structure, but also which components of the quadrupole moment tensor constitute the order parameter.

At first sight, neutron experiments do not seem well suited to probing quadrupole order because the neutron does not interact directly with electrostatic charge distributions. However, as was shown in the work of Effantin et al. on CeB_6 [1], this obstacle can be partly circumvented by concentrating on the response of the *dipole* moment lattice to a magnetic field applied along a high-symmetry direction in a single-crystal: indeed, this response is strongly constrained by the preexisting quadrupole order, and therefore contains relevant information, in the first place concerning the wave-vector of the quadrupole structure. We have applied this strategy to the magnetic semiconductor TmTe, which was recently reported to undergo a phase transition at $T_Q \sim 1.8$ K [2] (far above the Néel temperature of approximately 0.4 – 0.6 K) whose characteristics are suggestive of quadrupole order.

High-field measurements have been performed on the lifting detector diffractometer 6T2 using the Saclay-Grenoble 12-tesla split-pair cryomagnet, The data shown in Figure 1 clearly indicate that superstructure magnetic peaks associated with the zone-boundary wave-vector $\boldsymbol{k}$ = (1/2,1/2,1/2), which were absent in zero field, grow below T_Q as H is increased parallel to the [110] direction.

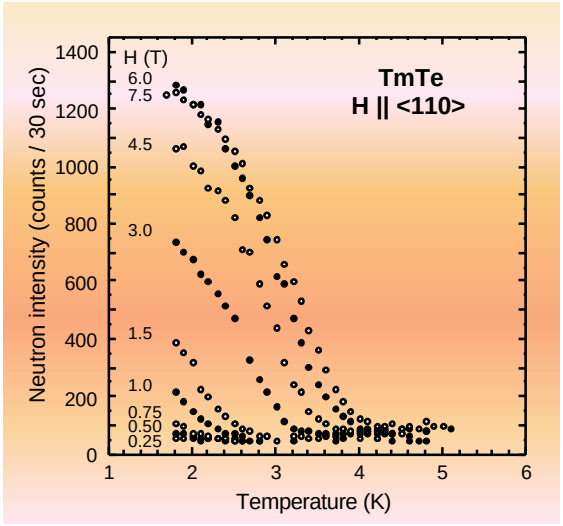

Figure 1. Intensity of the magnetic Bragg peak (3/2, -1/2, 1/2) induced by the external field H || [110].

This result is very important because it establishes the possibility for a *uniform* field to induce a *staggered* magnetic component in the ordered state below T_Q, whereas it induces only a component at $\boldsymbol{q}$ = 0 in the paramagnetic state. This lends considerable support to the above assumption of an underlying quadrupole order. By tracing these intensities as a function of temperature for different values of H, we were able to delineate the quadrupolar phase diagram for the three main symmetry directions, H || [001], [110], and [111] (Figure 2), and found good agreement with existing specific-heat results.

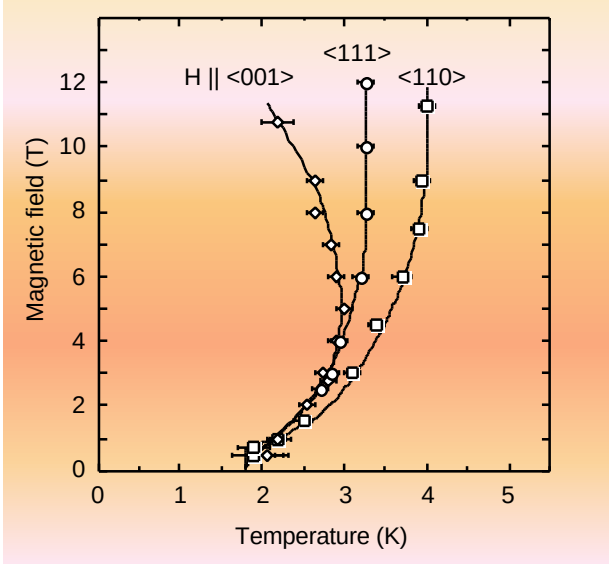

Figure 2. Quadrupolar phase diagram from the neutron diffraction results.

Furthermore, the quality of the data allowed us to fully disentangle the contribution of the different *k*- and *S*-domains, and to establish the direction of the staggered magnetic component μ_{AF} for H || [110], and [111]. In both cases, the best refinement was obtained by assuming μ_{AF} to be oriented along the two-fold axis $[1\bar{1}0]$ perpendicular to both the wave-vector $\boldsymbol{k}$ and the field direction. For H || [001], on the other hand, the induced magnetic component is much weaker and the direction of μ_{AF} cannot be reliably determined. Using the group-theoretical analysis developed by Shiina et al. [3], it can be concluded that the latter results are compatible with only one type of order parameter, namely O_2^2. A schematic illustration of the field response for H applied along (110) is given in Figure 3.

Recently, the measurements have been extended to temperatures around 0.1 K and it was found that the magnetic phase forming below T_N is of the canted type: it gives rise to two magnetic components, one antiferromagnetic with the same wave-vector $\boldsymbol{k}$ = (1/2,1/2,1/2) as the quadrupolar structure, and the other ferromagnetic. This effect had actually been predicted by Shiina et al. [3] for the case where "in-plane" magnetic couplings (*i. e.* bilinear interactions involving the x and y components of the dipole moment) dominate. Its experimental observation further supports the type of quadrupole order suggested above.

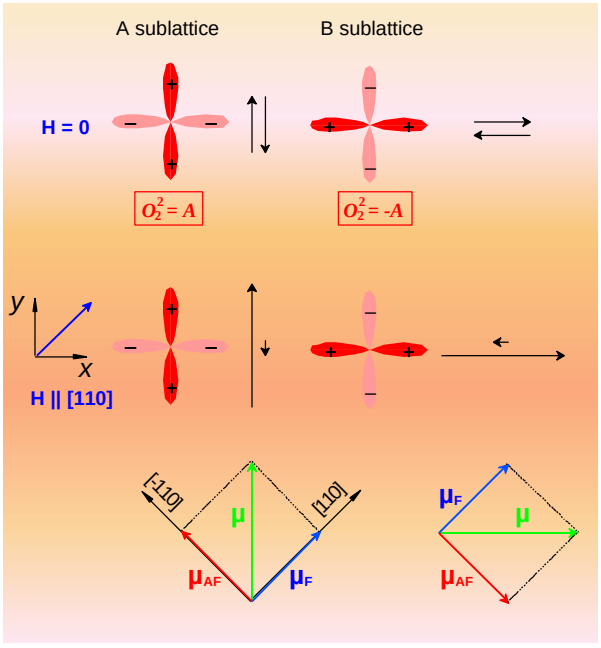

Figure 3. Schematic representation of the effect of a magnetic field H || [110] on the AFQ phase of TmTe; for H || [001], the symmetry is not broken and, ideally, only a uniform magnetic component is expected.

The results of this work [4] demonstrate that neutron diffraction, combined with a large external magnetic field, can provide a very powerful, albeit indirect, tool for studying quadrupole order in solids. Depending on systems, other techniques, such as synchrotron x-ray scattering may offer attractive alternatives. In the case of TmTe, however, the relatively low value of T_Q, as well as the risk of surface oxidation, make neutron diffraction the most straightforward method at the present time.

Further developments of this work, in particular measurements of the excitations in an applied field, will be aimed at clarifying the nature of the interactions responsible for the quadrupole ordering. Higher-order superexchange interactions have been suggested in Reference [3] but this assumption remains to be confirmed.

[1] J.M. Effantin, J. Rossat-Mignod, P. Burlet, H. Bartholin, S. Kunii and T. Kasuya, J. Magn. Magn. Mat. 47&48 (1985) 145.
[2] T. Matsumura, Y. Haga, Y. Nemoto, S. Nakamura, T. Goto and T. Suzuki, Physica B 206&207 (1995) 380.
[3] R. Shiina and H. Shiba, Physica B 259-261 (1999) 322.
[4] P. Link, A. Gukasov, J.-M. Mignot, T. Matsumura and T. Suzuki, Phys. Rev. Lett. 80 (1998) 4779.

MAGNETIC EXCITATIONS IN THE SPIN LADDER COMPOUNDS $Sr_{14-x}Ca_xCu_{24}O_{41+d}$

H. Moudden[1], L.P. Regnault[2], J.P. Boucher[3], L.E. Lorenzo[4], A. Revcolevschi[5]

[1]Laboratoire Leon Brillouin (CEA-CNRS)
[2]Département de Recherche Fondamentale sur la Matière Condensée, CEA-Grenoble, 38054 Grenoble cedex 9, France
[3]Laboratoire de Spectrométrie Physique, Université Joseph Fourier, BP87, 38042 Saint Martin d'Hères cedex, France
[4]Laboratoire de Cristallographie, CNRS Grenoble, BP.166, 38042 Grenoble, France
[5]Laboratoire de Chimie des Solides, CNRS URA 446, Université Paris Sud, Bât. 414, 91405 Orsay, France

At the boundary between dimensions one and two, spin-ladder systems are conceptually very interesting as they exhibit rather "exotic" properties. In particular, the spin-pairing expected to develop in a 2-leg ladder gives rise, upon doping, to a charge pairing and finally to a non conventional (i.e. non phonon mediated) superconductivity. In this report, we present recent neutron inelastic scattering results obtained on a single crystal of the undoped $Sr_{14}Cu_{24}O_{41+\delta}$ and doped $Sr_{14-x}Ca_xCu_{24}O_{41+\delta}$ 2-leg spin-ladder compounds.

After the discovery of the high-Tc superconductivity, a renewed interest in low-dimensional quantum magnetism has emerged, motivated by the possible role played by the magnetic interactions in the charge-pairing mechanism. One-dimensional antiferromagnets are particularly interesting to consider as they often exhibit unconventional phenomena. The first striking effect was discovered in the early 80's by Haldane[1], who suggested that Heisenberg antiferromagnetic chains with half-integer (S=1/2,3/2, ...) and integer (S=1, 2, ...) spin values behave quite differently at low temperatures. Whereas the former is expected to be gapless, the latter should have a non-magnetic singlet ground state and a quantum gap should open in the magnetic excitation spectrum. This non-intuitive prediction has been further very comprehensively verified from neutron-inelastic-scattering experiments performed on the spin-1 antiferromagnetic chain compound $Ni(C_2H_8N_2)_2NO_2ClO_4$.[2]. On the other side, the spin-1/2 square lattice with antiferromagnetic nearest-neighbour Heisenberg exchange couplings exhibits a quasi-ordered gapless ground state at T=0.
Spin-ladders can be viewed as an array of a finite number of coupled chains, allowing therefore to study the crossover between space dimensions 1 and 2. While spin ladders with an odd number of legs behave like the spin-1/2 antiferromagnetic chain (gapless excitation spectrum, power-law spin correlations, ...), those with an even number of legs exhibit an exponential decay of the spin-correlations due to the opening of a spin-gap (with energy A) in the excitation spectrum[3]. Of particularly high interest is the 2-leg spin-ladder system, since the prediction that charge doping could induce a non-conventional superconductivity, in which a d-wave pairing could be achieved, driven by the magnetic fluctuations[3]. Indeed, superconductivity has been recently discovered in the Ca-doped spin-ladder family $Sr_{14-x},Ca_xCu_{24}O_{41+\delta}$ for x>11, under high pressure in the range 30-45 kbar.[4] The understanding of the mechanism yielding to superconductivity in this material requires an accurate determination of both the temperature and doping dependencies of the magnetic excitation spectra. This can be achieved by neutron-inelastic- scattering investigations on undoped and doped single crystals.
As a first step, we have recently undertaken such a determination on the undoped $Sr_{l4}Cu_{24}O_{41+\delta}$ and doped $Sr_{14-x}Ca_xCu_{24}O_{41+\delta}$ compounds. The structure of this material is a misfit stacking of layers of two distinct quantum spin systems : linear CuO_2 chains and 2-leg Cu_2O_3 ladders[5]. Figure 1 shows a "3D" view of the crystallographic structure, which emphasizes the chain and ladder subsystems. Quite interestingly, the pure material contains a large amount of holes mainly localized in the CuO_2-chains (0.6 hole/Cu), which play the role of a charge reservoir.

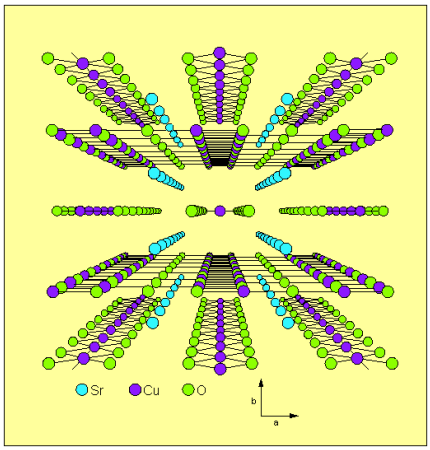

Figure 1: Crystal structure of $Sr_{14}Cu_{24}O_{41+d}$ showing the chain and ladder subsystems (viewed along the c axis).

Following the theoretical predictions, the ground state of a 2-leg spin-ladder system in the case $J_\perp < J_{//}$, where $J_{//}$ and $J_\perp$ represent respectively the exchange coupling constants along the legs and along the rungs, should be a non magnetic singlet ground state, well separated from the first excited states by an energy gap $\Delta \approx 0.4$

$J_\perp$. These two features have been unambiguously observed from neutron-inelastic-scattering experiments carried out on the 3-axes spectrometers (TAS) IN8/ILL, 1T/LLB and IN22/CRG-ILL. We show in Figure 2 two typical energy scans performed on TAS 1T/LLB at the scattering vectors **Q**=(4.5, 0, 0.5) (where one expects a strong signal originating from the ladders) and **Q**=(4.5, 0, 0.65) (where one expects a vanishing contribution of the ladders). The observed line shape is characteristic of a gapped magnetic response, with no signal detected at low energy and a gap value Δ=33 meV. The magnetic response can be understood from the existence of "two" contributions: one narrow contribution peaked at Δ and a second one, persisting at much higher energy and peaked around 40-50 meV. The temperature dependence of the magnetic response reveals several interesting and new features:

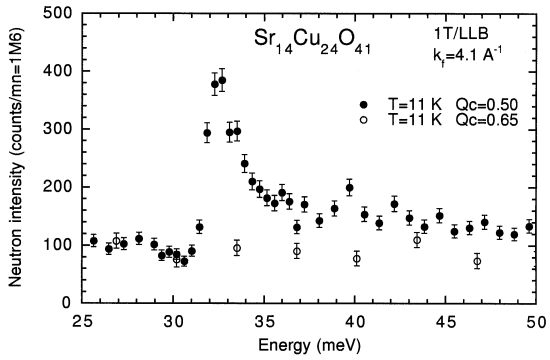

Figure 2: Inelastic neutron scattering response of the ladder subsystem at 1.5 K, showing the presence of a quantum spin-gap with energy 33 meV.

Figure 3: Dynamical magnetic response at 150K and 200K showing the existence of two distinct contributions in $Sr_{14}Cu_{24}O_{41+d}$

- the "33 meV-peak" disappears above roughly 200K, without strong renormalization nor damping below 150K. Figure 3 displays constant-Q scans at the scattering vector **Q**=(4.5,0,0.5) and two temperatures T=150K and 200K which demonstrate the presence of two distinct contributions.
- the second contribution is wealdy temperature dependent above 200K and extends at least up to 90 meV (data taken on IN1 and IN8/ILL).

We have presently no definitive explanation for these results, which however bear some ressemblance with those obtained on, e.g., $YBa_2Cu_3O_{6..5}$ in the normal state [6].

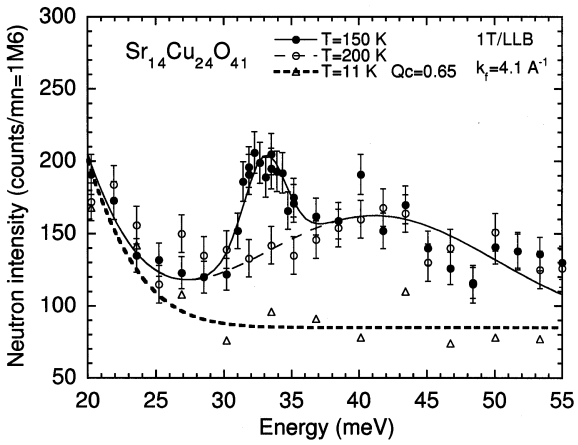

Upon Ca-doping, holes are progressively transferred from the CuO_2 chains to the Cu_2O_3 ladders which become metallic. Our neutron data show that the spin dynamics in the ladders is little affected by hole doping. The magnetic response, despite well visible broadening effects, remains peaked at 33 meV. At the reverse, the spin dynamics in the chain is much more affected, as a result of the partial destruction of the charge ordering in the chain subsystem.

References:

[1] F.D.M. Haldane, Phys. Lett. A**93** (1983) 464.
[2] L.P. Regnault, I. Zaliznyak, J.P.Renard and C. Vettier, Phys. Rev. B**53** (1994) 5579.
[3] E. Dagotto and T.M. Rice, Science **271** (1996) 618.
[4] M. Uehara, T. Nagata, J. Akimitsu, H. Takahashi, N. Môri and K. Kinoshita, J. Phys. Soc. Japan **65** (1996) 2764.
[5] E.M. McCarron, M.A. Subramanian, J.C. Calabrese and R.L. Harlow, Mat. Res. Bull. **23** (1988) 1355.
[6] P. Bourges et al, Phys. Rev. B**56** (1997) 1439.
[7] M. Matsuda, K. Katsurnata, H. Eisaki, N. Motoyarna, S. Uchida, S.M. Shapiro and G. Shirane, Phys.Rev. B**54** (1996) 12199
[8] L.P. Regnault et al, Phys. Rev. B**59** (1999) 1055.

NEUTRON SCATTERING FROM MAGNETIC EXCITATIONS IN $Bi_2Sr_2CaCu_2O_{8+d}$

H. F. Fong[1], P. Bourges[2], Y. Sidis[2], L. P. Regnault[3], A. Ivanov[4], G. D. Gu[5], N. Koshizuka[6] and B. Keimer[1,7]

[1] Department of Princeton University, Princeton, NJ 08544, USA.
[2] Laboratoire Léon Brillouin (CEA-CNRS)
[3] CEA Grenoble, DRFMC, 38054 Grenoble cedex 9, France.
[4] Institut Laue Langevin, 156X, 38042 Grenoble cedex 9, France.
[5] Department of Advanced Electronic Materials, University of New South Wales, Sydney 2052, Australia.
[6] SRL/ISTEC, 10-13, Shinomone 1-chome, Koto-ku, Tokyo 135, Japan.
[7] Max-Planck-Institut für Fertkörperforschung, 70569 Stuttgart, Germany.

Many of the physical properties of the copper oxides high-temperature superconductors appear to defy the conventional "one-electron" theory of metals. The development of alternative theories incorporating strong electron correlations is currently at the forefront of research in condensed matter physics. In this context inelastic neutron scattering can provide valuable insight into collective magnetic excitations in copper oxide superconductors and so guide these theoretical efforts.

For lack of suitably large single crystals, inelastic neutron scattering (INS) measurements have thus far proven possible for only two of the many families of high temperature superconductors, $YBa_2Cu_3O_{6+x}$ and $La_{2-x}Sr_xCuO_4$. While the magnetic spectra of both materials bear certain similarities, there are also pronounced differences that have hampered an unified description of the spin dynamics in the cuprates. In particular, the magnetic resonance peak that dominates the spectrum in the superconducting state of $YBa_2Cu_3O_{6+x}$, is not found in $La_{2-x}Sr_xCuO_4$.

In the optimally doped $YBa_2Cu_3O_{6+x}$ (superconducting transition temperature T_c=93 K), the magnetic resonance peak is a sharp collective mode that occurs at 40 meV and at the two-dimensional wave vector (π/a, π/a), where a is the nearest neighbour Cu-Cu distance (Fig.a). Its intensity decreases continuously and vanishes above T_c (Fig.b). In the underdoped $YBa_2Cu_3O_{6+x}$, the mode energy decreases monotonically with decreasing hole concentration. Such a collective excitation mode has not been observed in conventional superconductors. Several microscopic models have been proposed, ranging from band structure singularities to interlayer pair tunnelling. In all these models, the interactions that give rise to the resonance mode are the same that cause pairing of electrons in the superconducting state, so that this phenomenon provides a direct clue to the mechanism of high-T_c superconductivity.

A very sensitive test of the disparate models is whether they are capable of providing a detailed description of both the INS results and those of angle resolved photoemission measurements (ARPES), a complementary momentum resolved experimental technique that primarily probes single electron excitations. By far the best ARPES data have been obtained in $Bi_2Sr_2CaCu_2O_{8+\delta}$, a material for which no INS data have been available for experimental difficulties ($Bi_2Sr_2CaCu_2O_{8+\delta}$ cleaves easily along CuO_2 layers, which facilitates surface sensitive techniques such as ARPES, but this property is also responsible for the lack of large single crystal required in INS measurements). This situation that has precluded a direct quantitative comparison of both techniques is remediated by the present study.

We have performed the first INS measurements on a 60 mm^3 single crystal of $Bi_2Sr_2CaCu_2O_{8+\delta}$ (T_c=91 K). Measurements have been carried out on the triple-axis spectrometers 2T located at the reactor Orphée at Saclay and IN8 located at Institut Laue Langevin at Grenoble (France)

The magnetic excitation spectra of $Bi_2Sr_2CaCu_2O_{8+\delta}$ and optimally doped $YBa_2Cu_3O_{6+x}$ exhibit an unmistakable similarity. In the superconducting state, the magnetic intensity is sharply concentrated around a single point in energy (~43 meV, with a width of ~10-15 meV) and wave vector (**Q**=(π/a, π/a)) (Fig.c). In the normal state, the intensity is either too broad or too weak to be observable above background. Fig. d shows the temperature dependence of the peak amplitude which vanishes above the superconducting transition temperature to within the experimental uncertainty. There is also no indication of magnetic intensity above the background level at other energies or wavevectors. In particular, an extensive search for magnetic excitations at 10 meV has thus far been fruitless in $Bi_2Sr_2CaCu_2O_{8+\delta}$.

In both $Bi_2Sr_2CaCu_2O_{8+\delta}$ and $YBa_2Cu_3O_7$, the magnetic resonance peak is thus by far the most predominant feature in the magnetic excitation spectrum.

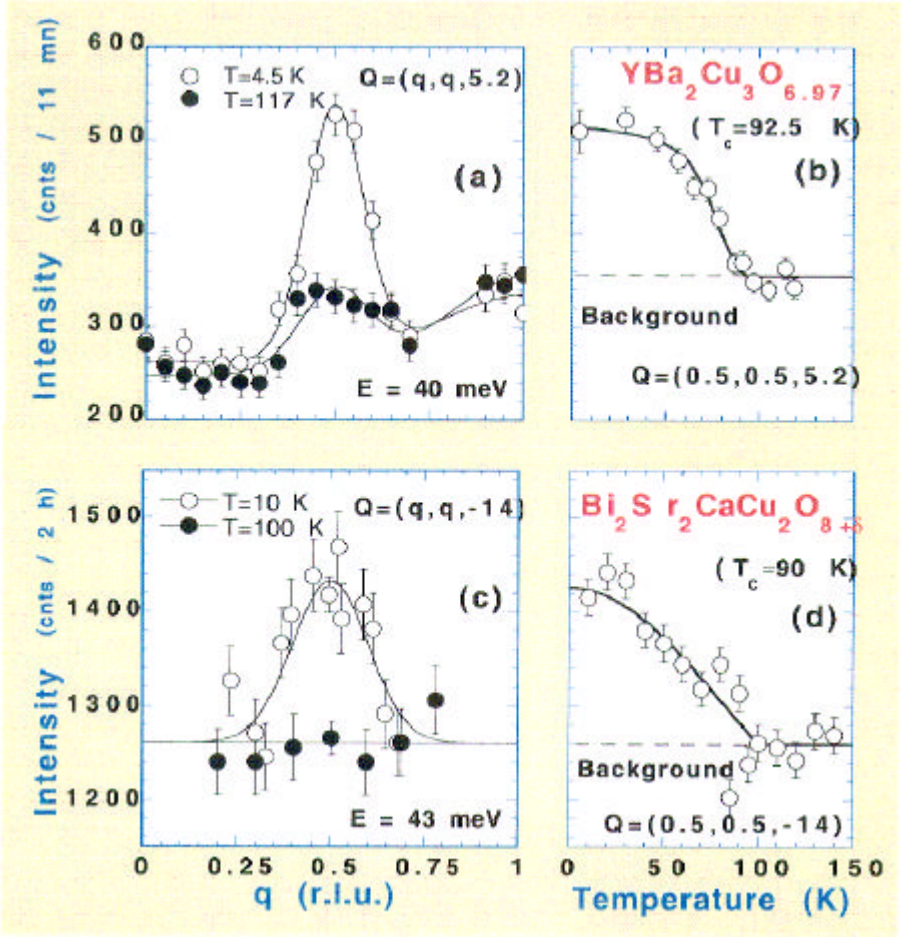

Figures : *Resonance peaks in $YBa_2Cu_3O_{6.97}$ (a,b) [E=40 meV] and $Bi_2Sr_2CaCu_2O_{8+d}$ (c,d) [E=43 meV]. The resonance peak is centered at the antiferromagnetic wave vector q = 0.5 (in reciprocal lattice units 2π/a). Its intensity vanishes above T_c (b,d)*

A further comparison between both compounds is made possible by a calibration of the absolute neutron cross-section against a vanadium standard. The energy integrated spectral weight of the resonance peak is 1.9±1 μ_B^2, in close agreement with 1.6 μ_B^2 found in $YBa_2Cu_3O_7$. The width of the resonance peak at the (π/a, π/a) wavevector is much larger in $Bi_2Sr_2CaCu_2O_{8+\delta}$ (0.53 $Å^{-1}$, full width at half maximum) than in $YBa_2Cu_3O_7$ (0.25 $Å^{-1}$). If averaged over the Brillouin zone, in addition to integrating over energy, the resonant spectral weight is clearly larger in $Bi_2Sr_2CaCu_2O_{8+\delta}$ (0.23 μ_B^2) than in $YBa_2Cu_3O_7$ (0.043 μ_B^2).
Such a quantitative comparison between different materials are required for a microscopic, quantitative description of the origin of the magnetic resonance peak. In the framework of the models proposed for the resonance peak, it should be now possible to relate the different Q-width measured in $YBa_2Cu_3O_7$ and $Bi_2Sr_2CaCu_2O_{8+\delta}$ to their different Fermi surfaces as measured by ARPES.

Our study opens the way to a variety of further neutron experiments, in particular in the overdoped regime which is easily accessible in $Bi_2Sr_2CaCu_2O_{8+\delta}$ over a wide range of hole concentrations. It has also left open questions that can only be answered by neutron scattering work on other families of high-T_C superconductors. For instance, as both $YBa_2Cu_3O_{6+x}$ and $Bi_2Sr_2CaCu_2O_{8+\delta}$ are bilayer materials, the present study does not provide further insight into the role of interlayer interactions in the resonance peak. Most importantly, the observation of the resonance peak in $Bi_2Sr_2CaCu_2O_{8+\delta}$ rules out the possibility that this phenomenon is due to a conspiracy of structural and chemical parameters in $YBa_2Cu_3O_{6+x}$. It is in fact an intrinsic feature of copper oxides superconductors and an explanation of this feature needs to be an integral part of any theory of high-temperature superconductivity.

References:

H. F. Fong, P. Bourges, Y. Sidis, L. P. Regnault, A.Ivanov, G. D. Gu, N. Koshizuka et B. Keimer, Nature **398**, 588 (1999)

OFF-SPECULAR REFLECTIVITY MEASUREMENTS ON PERIODIC MAGNETIC STRIPE DOMAINS IN $Fe_{0.5}Pd_{0.5}$ THIN FILMS.

B. Gilles[1], A. Marty[2], C. Fermon[3], F. Ott[4]

[1]LTPCM, ENSEEG, B.P.75, 38 042 Grenoble, France
[2]CEA-Grenoble, DRFMC, 17 rue des Martyrs, 38 054 Grenoble Cedex 9, France.
[3]Service de Physique de l'Etat Condensé, CEA-Saclay, 91191 Gif-sur-Yvette cedex
[4]Laboratoire Léon Brillouin (CEA-CNRS)

Specular polarised neutron reflectometry with polarisation analysis allows one to probe in-depth magnetic profiles of thin films (along the normal to the film). In the case of homogeneous films, the neutron is sensitive only to the in-plane magnetisation and all the intensity is reflected in the specular direction. In the case of non homogeneous films, all the directions of the magnetisation can be explored and intensity is scattered off the specular direction. The convention is to call « off-specular » the intensity measured in the incidence plane and « surface diffraction » the intensity measured out of the incidence plane. The incidence plane is defined by the incident wave vector and the perpendicular of the surface. Off-specular reflectometry gives information about lateral structures (in the plane of the film) with typical length scales ranging from 2 µm to 100 µm. Furthermore, surface diffraction at grazing angle gives access to transverse dimensions between 10 nm and 300 nm with a resolution in that direction of a few nanometers. The combination of these three types of signals (specular, off-specular and surface diffraction) applied to magnetic systems can lead to a 3D magnetic structure measurement. Off-specular measurements are however not applicable to the study of a single magnetic dot, but it can generate unique results in several cases including patterns of domain walls in thin films with perpendicular anisotropy, arrays of magnetic dots or patterned lines in magnetic thin films.

To demonstrate the potential of non-specular neutron scattering, we have measured magnetic surface diffraction on magnetic stripe domains appearing in FePd thin films. The sample was prepared by Molecular Beam Epitaxy under ultra-high vacuum (10^{-7} Pa). A 2 nm seed layer of Cr was deposited onto a MgO (001)-oriented substrate in order to allow the epitaxial growth of the 60 nm single crystal Pd buffer layer. A 50 nm thick FePd alloy layer was then deposited at room temperature using a mono-layer by mono-layer growth method in order to induce a chemical order similar to the one found in the tetragonal structure $L1_0$. This structure consists in alternate atomic layers of Fe and Pd on a body centred tetragonal lattice [1]. After a magnetisation along the easy axis, a magnetic stripe domain structure is observed [2] (see bottom picture on Figure 1).

The diffraction measurement has been performed using a small angle neutron scattering spectrometer (the spectrometer PAPOL at the Laboratoire Léon Brillouin) in a reflectivity configuration [3]. In the experiment, the stripes were aligned along the plane of incidence. An example of diffraction is shown on figure 1. One can observe a bright specular spot and two weaker (10^{-3}) off-specular peaks. The position of these peaks along the $q_{//}$ direction reflects the periodicity of the stripe domains (100 nm). The diffraction peaks are reflected with an angle θ_o equal to the critical angle θ_c of the layer whatever the incidence angle is.

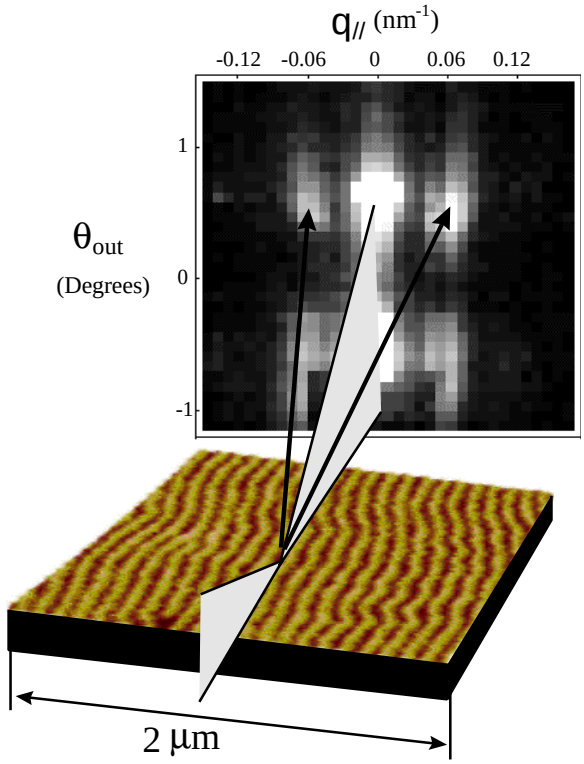

Figure 1 : diffraction geometry and off-specular scattering signal measured on a network of magnetic domains using a multidetector. The top peaks are the specular and off-specular peaks. The bottom signal is due to the refracted wave. The bottom picture is a Magnetic Force Microscopic image of magnetic domains observed in $Fe_{0.5}Pd_{0.5}$ thin films

The maximum intensity of the diffraction peaks is obtained when the incidence angle of the neutron beam on the sample is θ_c. These peaks have a behaviour similar to Yoneda peaks (or anomalous reflections) [4].

As a first approach, we have explained these observations by using a DWBA (Distorted Wave Born Approximation) approach. The considered « unperturbed » system is the flat FePd layer ; the perturbation is the magnetic structure created by the stripes. In this case, the diffuse cross-section can be written as [5] :

$$\left(\frac{d\sigma}{d\Omega}\right)_{diff} = (L_x L_y)\frac{\left|k_0^2\left(1-n^2\right)\right|^2}{16\pi^2}\left|T(\mathbf{k}_1)\right|^2\left|T(\mathbf{k}_2)\right|^2 S(\mathbf{q}_t)$$

with

$$S(q_t) = \iint_S dX\, dY\, C(X,Y)\exp\left(i\left(q_x X + q_y Y\right)\right)$$

(in the case where q_z^t is small) where *C(X,Y)* is the magnetic roughness correlation function, **q** is the scattering vector $\mathbf{k}_2$-$\mathbf{k}_1$ and $\mathbf{q}_t$ is the wave-vector transfer in the medium. Maxima are obtained in the diffuse scattering when $\mathbf{k}_1$ or $\mathbf{k}_2$ makes an angle close to q_c since in these positions, the Fresnel coefficients **T** reach a maximum.
$S(\mathbf{q}_t)$ is the Fourier transform of the magnetic roughness correlation.
In the case of our magnetic lines, we define the correlation function of the magnetic roughness as :

$$C(X,Y) = \frac{1}{S}\iint_S M(x,y)M(x+X,y+Y)dxdy$$

The surface diffraction signal measures the Fourier transform of the magnetic correlation function. The figure 2 shows the off-specular signal calculated for an incidence angle equal to the critical angle $\theta_i=\theta_c=0.5°$. The peak positions are unchanged whatever the incidence angle is. The maximum of intensity is obtained when the incidence angle is equal to the critical angle θ_c.
The DWBA approach is however not well suited to this problem since the magnetic roughness extends over the full thickness of the magnetic layer so that the flat layer as a basis state is far from the real eigenstates of the system. We are presently working on a fully dynamical theory to be able to quantitatively analyse magnetic off-specular patterns.

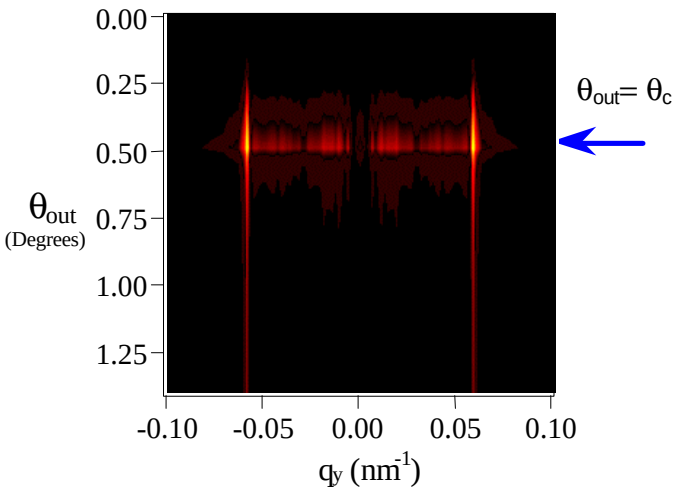

Figure 2 : calculated off-specular signal as measured on a multidetector for an incidence angle $q_{inc} = q_c = 0.5°$. The peaks maximum position does not move when the incidence angle is varied but the intensity decreases as soon as the incidence angle is moved away from the critical angle θ_c.

We hope that this work will pave the way for a new technique of 3D magnetometry making it possible to measure quantitatively magnetic structures with an in-depth and in-plane resolution. The aim is to eventually be able to obtain magnetic information on the magnetic order in the plane of thin films through polarised neutron reflectometry. Off-specular and surface diffraction will then make it possible to probe in-plane magnetic structures of sizes ranging from 10 nm to 100 µm.

References

[1] V. Gehanno, A. Marty, B. Gilles and Y. Samson, Phys. Rev. B **55** (1997) 12552.
[2] A.L. Sukstanskii, K.I. Primak, J. Magn. Magn. Mater. **169** (1997) 31.
[3] C. Fermon, F. Ott, B. Gilles, A. Marty, A. Menelle, Y. Samson, G. Legoff and G. Francinet, Physica B **267-268** (1999) 162-167.
[4] Y. Yoneda, Phys. Rev. **131** (1963) 2010 ; O.J. Guentert, J. Appl. Phys. **30** (1965) 1361 ; A.N. Nigam, Phys. Rev. A **4** (1965) 1189.
[5] S.K. Sinha, E.B. Sirota, S. Garoff and H.B. Stanley, Phys. Rev. B **38** (1988) 2297-2311.

NEW SCENARIO FOR HIGH-T_c CUPRATES : ELECTRONIC TOPOLOGICAL TRANSITION AS A MOTOR FOR ANOMALIES IN THE UNDERDOPED REGIME

F. Onufrieva , P. Pfeuty, M. Kisselev and F. Bouis

Laboratoire Léon Brillouin (CEA-CNRS)

This is a particularly exciting time for high-T_c. The experimental knowledge converges. Almost all experiments, nuclear magnetic resonance (NMR), angle resolved photoemission spectroscopy (ARPES), tunneling spectroscopy etc., provide an evidence for the existence of a characteristic energy scale $T^*(\delta)$ in the underdoped regime (δ is hole doping). Below and around the line $T^*(\delta)$ the "normal" state (i.e. above T_c) has properties fundamentally incompatible with the present understanding of metal physics. The field has reached the point when a consistent theory is needed to understand this experimentally well defined but theoretically exotic metallic behaviour and its relevance to high T_c superconductivity.

We show that these phenomena can be naturally understood within the concept of a proximity of the underdoped regime to an electronic topological transition (ETT). The concept of electronic topological transition due to the variation of the topology of the Fermi surface was introduced in the early 60's by I. Lifshitz and applied to 3D systems [1]. It was shown that an ETT implies singularities in thermodynamic and transport properties at T=0 which are smoothed at finite temperature (this left Lifshitz in a difficult position concerning the classification of this transition as a phase transition). Due to (i) the weakness of the singularities in 3D case (the only dimension considered at Lifshitz's time) and (ii) the difficulty of classification, this phenomenon (which is as general as for example the phenomenon of phase transition) has been quite forgotten.

We analyse a 2D electron system on a square lattice (in direct application to the high-T_c cuprates) and show that it obligatory undergoes an ETT (the Fermi surface changes from open to closed) under change of electronic concentration n (or of hole doping δ=1-n) and that the ETT occurs in the doping range where all anomalies in the high-T_c cuprates are observed. We show that the ETT point, $\delta = \delta_c$, T = 0, is a quantum critical point (QCP) (at Lifshitz's time the concept of QCP had not yet been introduced), which is very rich in the 2D case, and that its existence results in global anomalies of the system[2-6]. Firstly, in the presence of interaction of necessary sign (such interaction does exist in the strongly correlated CuO_2 plane being of magnetic origin, see [7]), a d-wave superconducting state with high T_c develops around the ETT QCP with maximum T_c at $\delta = \delta_c$; its symmetry and properties studied in [7] are in a good agreement with experiments. Secondly, the underdoped regime, $\delta < \delta_c$ above $T_{sc}(\delta)$ is a new type of metallic state: quantum spin-density wave (SDW) liquid re-entrant in temperature and frozen in doping [4,2]. The re-entrance means that the characteristics of the short range order behave in a re-entrant way: the system becomes more ordered with increasing T and it reaches a minimum disorder at some pseudocritical temperature $T^*(\delta)$ which increases with decreasing doping. Freezing means that the system keeps strong short range order (or strong quantum critical fluctuations) quite far in doping from the ETT QCP.

A detailed study of these phenomena allows to understand many effects observed in high-T_c cuprates by different experiments and unexplained until now. Below we present several examples of theoretical predictions of our theory. Notice that the different anomalies are explained within the same theory and that neither adjustable parameters nor phenomenological *anzatz* are used.

Nuclear magnetic resonance (NMR)

There are two glaring anomalies observed systematically in the underdoped high-T_c cuprates; (i) the nonmonotonical behaviour of the nuclear spin lattice relaxation rate $1/T_1T$ on copper with maximum at some T* (see Fig.1b) instead of the Korringa law $1/T_1T$=const for ordinary metals, (ii) qualitatively different behaviour of $1/T_1T$ measured on copper and oxygen (or for the wavevectors $\mathbf{q} \approx \mathbf{Q}_{AF}$ and $\mathbf{q} \approx 0$ from theoretical point of view), see Fig 1d. (The relaxation rate $1/T_1T$ is roughly proportional to the slope in the imaginary part of the spin dynamic susceptibility, $\lim_{\omega\to 0} \mathrm{Im}\chi^0(\mathbf{q},\omega)/\omega$). The results of our theory are in a very good agreement with experiment, compare Fig.1a and 1b (there are no adjustable parameters). The shown dependences are a manifestation of the quantum SDW liquid : the nonmonotonic behaviour reflects the re-entrance in T. The difference in behaviour for $\mathbf{q} \approx \mathbf{Q}_{AF}$ and $\mathbf{q} \approx 0$ is related to the different aspects of criticality of the ETT QCP. The detailed analysis is done in [4].

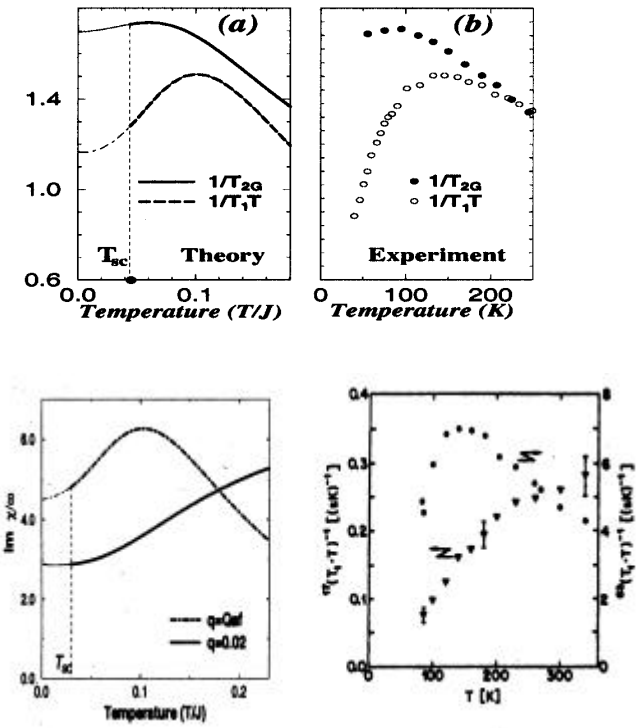

Figure 1. Comparison between theory and experiment for $1/T_1T$ on copper and oxygen. (a) and (b) show the $1/T_1T$ and $1/T_{2G}$ (nuclear transverse relaxation rate) on copper, (a) calculated [2,4] (should be considered only above T_{sc}) and (b) measured by NMR for $YBCO_{6.6}$ [8]; (c) and (d) demonstrate the qualitatively different temperature dependences for copper ($\mathbf{q} \approx \mathbf{Q}_{AF}$) and oxygen ($\mathbf{q} \approx 0$): (c) shows the theoretical results nonintegrated in $\mathbf{q}$ (the function for $\mathbf{q} \approx 0$ is multiplied by factor 20), (d) shows experimental data for $1/T_1T$ on copper (Cu^{63}) and on oxygen (O^{17}) in $YBa_2Cu_4O_8$ [9].

Angle resolved photoemission spectroscopy (ARPES)

There are numerous anomalies observed by photoemission in the underdoped regime (ARPES directly measures the electron spectral function as a function of energy and wavevector) which can be summarized as the so-called $(\pi,0)$ feature : the Fermi surface disappears in the normal state in the vicinity of $(\pi, 0)$ wavevector while in all ordinary metals it is well defined; the spectrum has a very unusual flat form as a function of wavevector; the electron spectral function $A(\mathbf{k}, \omega)$ is almost non-structured as a function of energy with a hump in the normal state and with the peak-dip-hump in the superconducting state instead of the usual almost δ-function form, etc. Within our theory all anomalies find a natural explanation. They are signatures of the quantum spin density wave (SDW) short range ordered liquid state, being a precursor of the ordered SDW phase. For example, the spectrum shown in Fig.2a, 2b is a result of a hybridization of the two parts of the bare spectrum in the vicinity of two different saddle points $(0,\pi)$ and $(\pi,0)$. The bare spectrum (dashed line) splits into two branches, $\varepsilon_1(\mathbf{k})$ and $\varepsilon_2(\mathbf{k})$. The hybridization is static for the ordered SDW phase and is dynamic for the disordered (quantum SDW liquid) state. In the latter case the mode $\varepsilon_2(\mathbf{k})$ is strongly damped and appears above an incoherent background. The spectrum is in excellent agreement with ARPES data, see Fig.2c (ARPES measures only the part corresponding to negative energies ω). The existence below Fermi level of the incoherent background and of the damped mode $\varepsilon_2(\mathbf{k})$ explains the anomalous almost nonstructured ω dependence of the electron spectral function with the hump at energy $\approx \varepsilon_2(\pi,0)$ observed experimentally above T_{sc}. The effect of splitting into two branches leads to the pseudogap opening. The behaviour as a whole is strikingly similar to that observed experimentally. It concerns the very existence of pseudogap below T^*_{gap} which grows with decreasing δ, its doping and temperature dependences, the gradual disappea-rence of the Fermi surface with T, the shape of the spectrum around $(0,\pi)$, etc. Details are given in [3].

These were the features existing at intermediate temperature (above T_{sc}). At low temperature, the general picture of the spectrum is the same except that the upper branch $\varepsilon_1(\mathbf{k})$ (i) moves to lower energies and intersects the Fermi level [3], (ii) gets a gap, $E_1^{\pm}(\mathbf{k}) = \pm\sqrt{\varepsilon_1^2(\mathbf{k}) + \Delta^2(\mathbf{k})}$ in the presence of superconductivity with $\Delta(\mathbf{k}) = \Delta(\cos(k_x) - \cos(k_y))$ for the d-wave symmetry. Therefore two modes exist below Fermi level: the well- defined $E_1^-(\mathbf{k})$ and

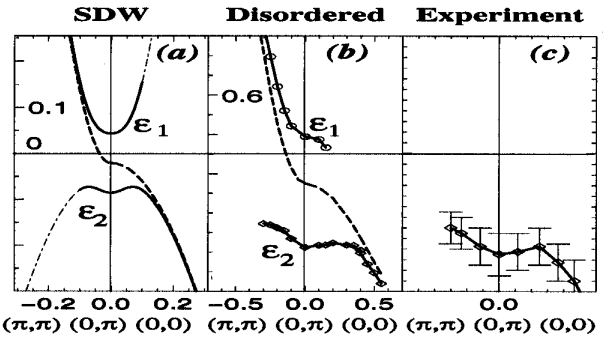

Figure 2. Electron spectrum $e(\mathbf{k})/t$ as a function of wavevector along G - X symmetry lines in the Brillouin Zone, (a) in the ordered SDW phase, (b) in the quantum SDW liquid state above T_{sc}. (c) ARPES data[10] for underdoped BSCO above T_{sc}. The dashed lines correspond to the bare spectrum, the thick lines to the two branches of the splitted spectrum, the dot-dashed line in (a) to the spectrum with the spectral weight less than 0.1.

the strongly damped $\varepsilon_2(\mathbf{k})$ which leads to the peak-dip-hump form of $A(\mathbf{k},\omega)$ as a function of ω observed experimentally in the superconducting (SC) state (E_1 corresponds to the peak and ε_2 to the hump).

Tunneling spectroscopy

The typical form of the tunneling function with peak-dip-hump features at negative energies, $\omega<0$ as well as the asymmetry between $\omega<0$ and $\omega>0$ observed experimentally (see Fig.3b) and not understood until now are also explained well by our theory, compare Fig.3a and 3b. The effects are direct consequences of the discussed above form of the electron spectrum in the quantum SDW liquid state (tunneling spectroscopy measures the density of states, i.e. the electron spectral function integrated in $\mathbf{k}$). The peak-dip-hump structure seen in Fig.3 at negative ω results from the existence of two modes below the Fermi level (FL). So far, as it is not the case above FL, the picture in ω is quite asymmetrical.

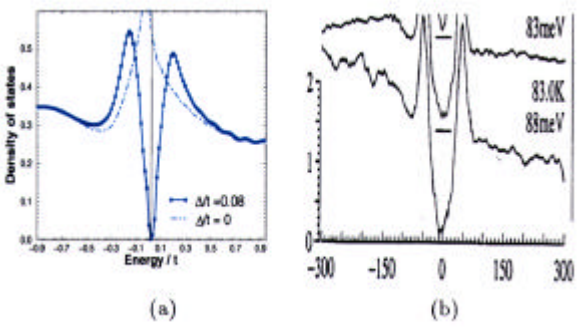

Figure 3. The density of states (a) calculated in the normal state (dotted line) and in the superconducting state (full line), (b) measured by tunneling [11] at T=4.2K: the lowest curve corresponds to the underdoped Bi2212 (T_c=83K); the energy scale is given in meV.

Inelastic neutron scattering (INS)

The existence of the quantum SDW liquid state and of the corresponding quantum spin fluctuations have a direct consequence for the spin dynamics measured by INS. Firstly, it explains the very fact of magnetic response so strong that it can be measured by INS (in ordinary metals it is impossible). Secondly, it explains practically all details observed by INS. Most interesting among the theoretical predictions are maybe the existence in the SC state (i) of the resonance spin mode (with almost horizontal dispersion in the vicinity of $\mathbf{Q}_{AF}$) developing out of two particle electron-hole continuum and (ii) of the incommensurability at low energies[5]. The former explains well the resonance peak at $\mathbf{q}=\mathbf{Q}_{AF}$ and $\omega \approx$ 40 meV with resolution-limited energy width and a finite q width observed systematically in the SC state from the beginning of high-T_c era[12]. The latter explains recent results obtained with a high resolution spectrometer, see Fig.4b[13]. The agreement with experiment is remarkable, compare Fig.4a and 4b.

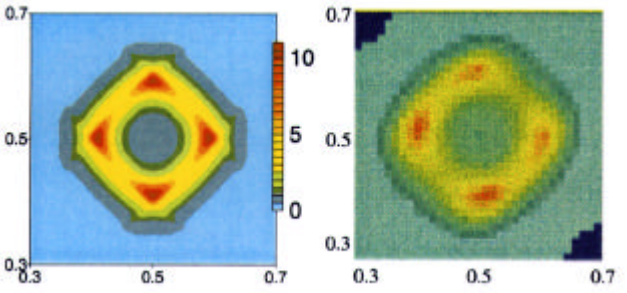

Figure 4. $\mathbf{q}$ dependence of Imc($\mathbf{q}$,w) (a) theoretical for w/J = 0.25, (b) experimental [13] ($YBCO_{6.6}$ for w = 25 meV). The point (0.5,0.5) corresponds to (π/a,π/a). Note that J »120 meV for the cuprates.

References

[1] I.M. Lifshitz, Sov.Phys.JETP. **11**, 1130 (1960)
[2] F.Onufrieva, P.Pfeuty, M. Kisselev, Phys.Rev.Lett. **82**, 2370 (1999)
[3] F.Onufrieva, P.Pfeuty, Phys.Rev.Lett. **82**, 3136 (1999)
[4] F.Onufrieva, P.Pfeuty, Phys.Rev. B, (1999), to appear
[5] F.Onufrieva, P.Pfeuty, cond-mat/9903097
[6] F.Bouis, M.Kisselev, F.Onufrieva and P.Pfeuty, cond-mat/9906369
[7] F.Onufrieva, S.Petit, Y.Sidis, Phys.Rev.B, **54**, 12464 (1996)
[8] M. Takigawa, Phys.Rev.B, **49**, 4158 (1994)
[9] C.Berthier et al, J. de Phys I France, **6**, 2205, (1997)
[10] D.S. Marshall et al, Phys.Rev.Lett., **76**, 4841 (1996)
[11] Ch. Renner et al, Phys.Rev.Lett., **80**, 149 (1998)
[12] J.Rossat-Mignod et al, Physica C, **185-189**, 86 (1991); H.F. Fong et al, Phys.Rev.Lett. **78**, 713 (1997); P. Bourges et al, Europhys.Lett. **38**, 313 (1997)
[13] H.A. Mook et al. Nature, **395**, 580 (1998)